Korean J. Chem. Eng., 33(10), 2968-2981 (2016)
DOI: 10.1007/s11814-016-0154-y

pISSN: 0256-1115
eISSN: 1975-7220

Self-cleaning behavior of nanocomposite membrane induced by photocatalytic WO_3 nanoparticles for landfill leachate treatment

Nader Shafaei, Mohsen Jahanshahi, Majid Peyravi†, and Qasem Najafpour

Membrane Research Group, Nanobiotechnology Institute, Babol University of Technology, Babol, Iran
(*Received 15 February 2016 • accepted 8 June 2016*)

Abstract−Photocatalytic self-cleaning polysulfone (PSf) membranes were fabricated by adding different concentrations of WO_3 nanoparticles (0-2 wt%) via phase inversion method for ultrafiltration of landfill leachate. To evaluate the feasibility of self-cleaning property by WO_3 nanoparticles, all synthesized membranes were tested with and without UV. After UV irradiation, the value of the contact angle for a membrane with 2 wt% WO_3 decreased from 67.15° to 37.9°. Results showed that the addition of WO_3 affected the pore size, porosity and hydrophilicity of the WO_3/PSf membrane, so that the porosity of membrane with 2 wt% WO_3 reached 84.86%. The flux of the nanocomposite membrane after irradiation by UV light rose in comparison with the same membrane without UV light, and the flux decline rates also decreased. The flux of the membrane with 2 wt% WO_3 was also better than the other membranes, which shows the self-cleaning property. The chemical oxygen demand (COD) removal of leachate for modified membranes was also improved by increasing the WO_3 nanoparticles. The highest COD removal of the modified membrane with 2 wt% WO_3 was 54.91%. This value increased to 77.45% after UV radiation.

Keywords: Self-cleaning Property, Leachate Treatment, WO_3 Nanoparticle, Polysulfone, Nanocomposite Mmembrane, UV Light

INTRODUCTION

The common incorporated membranes used in the separation processes are polymeric membranes because of their favorable characteristics such as desired film forming ability, toughness, low cost and their ease of integration with other processes [1,2]. Among a wide range of polymers, the sulfone polymer family, especially polysulfone (PSf), known as a suitable material, has been used in producing various types of ultrafiltration (UF) membranes because of their low cost, good mechanical properties, good anticompaction properties, thermal stability and alkaline resistance. Although the mentioned properties are appropriate, PSf has some undesirable properties such that if these are resolved, the PSf membrane will be proper for wastewater treatment [3]. A PSf exhibits two main disadvantages: (i) a hydrophobic nature which intensifies the membrane fouling and consequently permeability reduction [4], and (ii) the problem of coating the PSf support with polymers which are only soluble in organic solvents [5].

One of the major concerns in the operation of the various separations by membrane process is fouling [6]. Fouling is the blockage of membrane pores during filtration, which is caused by the combination of sieving and adsorption of particles and compounds onto the surface of membrane or within its pores [7]. Membrane fouling can either be reversible (deposition of retained solutes on the surface of the membrane as a gel cake layer) [8] or irreversible (adsorption or pore plugging of solutes in and within the membrane pore matrix) [7]. The approaches taken for preventing membrane fouling are classified in three groups: i) Modifying the feed by using pretreatments such as adsorption, coagulation or flocculation [9]; ii) Modifying the hydrodynamics of the membrane surface to improve the concentration polarization [10]; and iii) Modifying the membrane surface by adding desirable materials [11]. The present work is focused on the modification of the PSf ultrafiltration membrane to understand the concept of the fouling mechanism based on the experimental observation.

To achieve a more hydrophilic membrane surface, there are several methods such as graft polymerization with hydrophilic polymers, monomers or functional groups [12], plasma treatment [13], physical adsorption [14], γ-ray-induced graft polymerization [15], polymer blending [16] and embedding hydrophilic nanoparticles to a membrane structure [17]. This makes antifouling membrane which the foulants will not adsorb or will be cleaned by physical methods easily [18]. Using nanoparticles such as TiO_2, ZnO, Fe_2O_3, ZrO_2 and ZnS on membrane structure not only improves the membrane antifouling properties [19], but also develops a membrane with self-cleaning properties [20]. Recently, self-cleaning coatings have received significant attention in academic research because of their extensive applications [21,22]. The self-cleaning coating is usually divided into hydrophilic and hydrophobic coatings. It also has some advantages such as reduction in maintenance costs and time spent on cleaning surface [23]. These nanoparticles can decompose organic chemicals in the environmental liquid waste by their photocatalytic and superhydrophilicity effects. In recent researches, photocatalysis has focused on these semiconductor materials for the removal of organic and inorganic species from aqueous or gas phase systems in environmental cleanup, drinking water treatment,

†To whom correspondence should be addressed.
E-mail: majidpeyravi@gmail.com
Copyright by The Korean Institute of Chemical Engineers.

industrial and health applications [24]. A self-cleaning process usually contains two stages; organic and inorganic materials are deposited on the surface in the first stage, and followed by the layer of water cleans the membrane surface because of the super-hydrophilicity at the second stage [25]. WO_3 is one of semiconductor metal oxides that has emerged as the photocatalyst material for environmental purification due to its desired band gap energy, nontoxicity and stability [26]. WO_3 has attracted most of the attention because of their low cost, ease of preparation, smooth morphology and high stability in aqueous solution [27,28]. In the present research, the feasibility of WO_3 to create photocatalytic and superhydrophilicity properties in the PSf membrane is assessed. For this purpose, WO_3 nanoparticles were incorporated in the membrane structure through dispersion in the polymer dope solution. The self-cleaning property of the membrane was studied after UV radiation. Further, fouling studies by leachate as a case study were carried out to understand the effect of self-cleaning on the membrane long-term performance.

MATERIALS AND METHODS

1. Materials

Polysulfone (PSf) pellets supplied by Udel P-1700 NT LCD were used for UF membrane forming material, and N,N-dimethylacetamide (DMAc) as solvent was provided by BASF Co. (Germany). Polyethylene glycol (PEG) with molecular weight of 600 Dalton as the viscosity adjustment and the dispersant agent was purchased from Merck. WO_3 and Ammonium peroxydisulfate (APS) were used with analytical grade.

2. Feed

Landfill leachate used in this study was obtained from a landfill leachate waste municipal site located in Kiasar region of Sari, Mazandaran province, Iran. Lists of the characteristics of the raw leachate are given in Table 1. These characteristics were measured according to the standard methods [29].

3. Membrane Preparation

PSf membranes were prepared by the immersion phase inversion method. Casting solution was prepared by dispersing WO_3 in DMAc and the dispersion was sonicated for about 30 min using an ultrasonic device. Then PSf was dissolved in the aforementioned solution with magnetic stirring at 200 rpm to prepare PSf/WO_3 solutions with different composition. Also, 2 wt% PEG as a viscose agent was added to the casting solution at ambient temperature. In all dope solutions, the mass ratio of PSf to solution was set 16 wt% and WO_3 mass ratio was varied from 0-2 wt% (0, 0.5, 1 and 2 wt%). The homogeneous polymer solution was left overnight without stirring to allow complete release of bubbles. The solution was cast by film applicator on polyethylene/polypropylene non-woven fabric. The thickness of the ultrafiltration membrane was adjusted to 75 μm through adjusting the position of the casting knife and then immersed in a coagulation bath of pure water. The prepared membrane was kept overnight in the water bath to completely leach out the residual solvents and additives. Finally, the membrane was placed between two paper filters for drying completely.

Table 1. Physico-chemical characteristics of raw landfill leachate

Parameter	Concentration
pH	8-8.3
Alkalinity (mg/L as $CaCO_3$)	7300-7500
Suspended Solids (SS)	2500-2700
Biochemical oxygen demand (BOD) (mg/L)	910
COD (mg/L)	12420
Total Kjeldhal nitrogen (mg/L)	3300
Total phosphorus (mg/L)	2300
NO_3-N (mg/l)	640
Total dissolved solids (TDS) (mg/ml)	7.8
Conductivity (ms/cm)	15.5

4. Membrane Characterization

Chemical structure of membranes was measured by the attenuated total reflection (ATR) technique using Bruker-IFS 48 FTIR spectrometer (Ettlingen, Germany) with the horizontal ATR device (Ge, 45°). The morphology of the membranes was examined by scanning electron morphology (SEM) and atomic force microscopy (AFM). SEM analyses were utilized to characterize the morphology and surface of membranes by Philips (Philips-X130). The elemental composition of membrane surfaces was conducted using an EDS X-ray detector equipped by the scanning electron microscopy. The AFM device was Nanosurf scanning probe-optical microscope (EasyScan II, Swiss). Surface topography and surface roughness of the membranes were analyzed using AFM images and calculated by a tapping mode method via Nanosurf EasyScan software at a scan area of 5 μm×5 μm, respectively. To characterize the property of hydrophilic polymeric surfaces, contact angle measurement was used. The contact angle between water and the membrane surface in this research was measured with Dataphysics-OCA 15 plus. Deionized water was used as the probe liquid in all measurements. To investigate the effect of UV light on hydrophilicity, the modified membrane illuminated by UV lamp for 10 min [30] at the distance of 5 cm, was measured by contact angle. The contact angle of the neat membrane was also measured and compared to the modified one.

5. Porosity and Pore Size Measurements

Generally, membranes should have high surface porosity and good pore structure to obtain high permeability. Porosity (ε_m) is defined as the membrane void volume/total volume, and specific surface area. It was determined by immersing the membrane in the DI water overnight at room temperature. The excess water on the membrane surface was removed by filter paper, and the thickness was measured by a digital micrometer. The weight of the membrane before and after wetting in the DI water was determined. Therefore, the porosity was calculated according to the following equation [31]:

$$\varepsilon(\%) = \frac{W_w - W_d}{\rho \cdot A \cdot l} \times 100 \quad (1)$$

where W_w (g) and W_d (g) are the weights of the wet and dry membranes, A (m^2) is the membrane area, ρ (kg/m^3) is the pure water density and l (m) is the membrane thickness.

The pore radius of the membrane was also determined on the

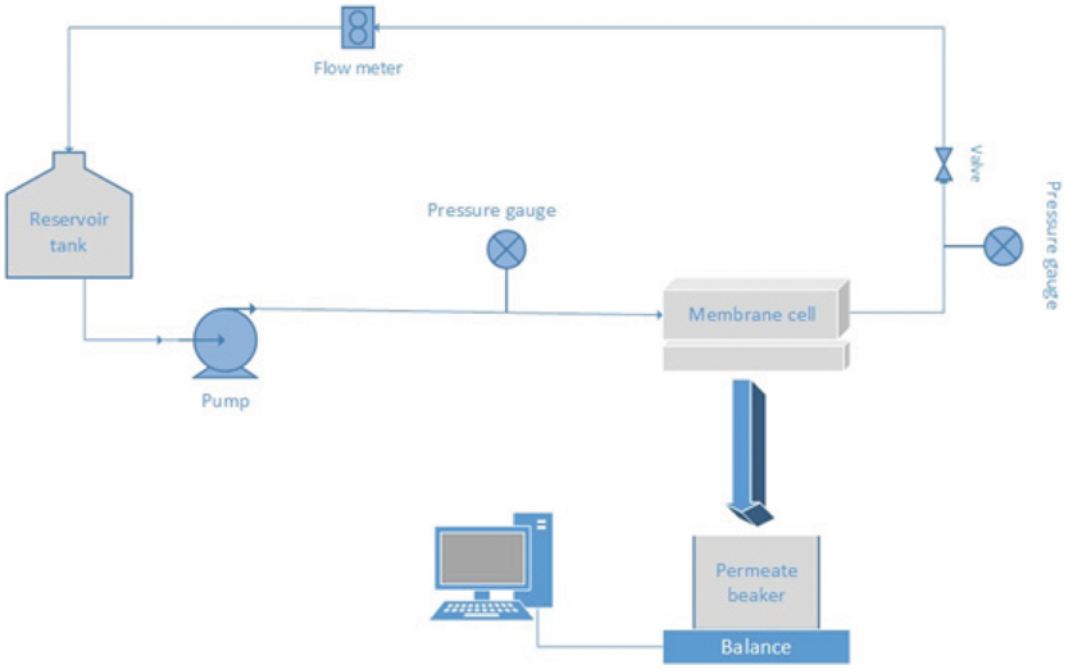

Fig. 1. A schematic diagram of reverse osmosis system.
1. Reservoir tank 2. Pump 3. Pressure gauge 4. Membrane cell 5. Permeate beaker 6. Valve 7. Flow meter

basis of the pure water flux and porosity data by Guerout-Elford-Ferry equation [32]:

$$r_p = \sqrt{\frac{(2.9-1.75\varepsilon)\cdot 8\cdot \eta\cdot l\cdot Q}{\varepsilon\cdot A\cdot \Delta P}} \quad (2)$$

where η is the water viscosity (8.9×10^{-4} Pa·s), Q (m^3/s) is the volume of the permeate pure water per unit time, ε is porosity, l (m) is the membrane thickness, A (m^2) is the membrane area and ΔP is the operating pressure (3×10^5 Pa).

6. Testing Protocols

Membrane filtration experiments were performed to utilize a laboratory-scale cross flow filtration setup, which is shown in Fig. 1. It contains a 10 L feed reservoir, a high pressure diaphragm pump, a membrane cell with an effective area of 63.25 cm^2, valves, a pressure gauge, a flow meter and a heat exchanger. The operating conditions of the experiments were also constant at the transmembrane pressure of 3 bar and temperature of 25±1 °C. The feed flow rate was controlled and fixed at 621.76 *l*/hr.

For radiation of membranes with ultra-violet (UV) light, a 125 W (300 nm<λ<400 nm), UV light (Osram, Germany) was utilized. To investigate the self-cleaning effect of the membrane surface, the membrane was washed in distilled water and illuminated by UV lamp for 10 min at the distance of 5 cm at the intensity of 3.98×10^2 mW/cm^2. Then the treated membrane was kept in distilled water for 15 minutes before being tested in the experiment. The self-cleaning process usually contains two steps: the absorbed contaminants on the surface are decomposed by the photocatalysis in the first steps, followed by the water sheeting action due to superhydrophilic surface in the second step. In the present research by choosing the WO_3 nanoparticles both steps were done in the presence of UV light. The flux (J), through the membrane, can be described by the following equation:

$$J = \frac{V}{A\ \Delta t} \quad (3)$$

where V is volume of permeate, A is the membrane area and Δt is the permeation time. To deal with the long term test, permeation flux was calculated every 15 minutes during long term filtration. Further, the rate of flux decline (K), was measured by the equation below [33]:

$$k = \frac{-1}{Q}\left(\frac{dQ}{dt}\right) \quad (4)$$

The chemical oxygen demand (COD) removal percentage in the permeate was calculated using the following equation:

$$\text{COD Removal (\%)} = \left(1-\frac{C_p}{C_f}\right)\times 100 \quad (5)$$

where C_p and C_f (mg/ml) were the COD of permeate and feed, respectively. To measure the COD of feed and permeate, the samples were micropipeted into the COD digestion solution vials. The vials were sealed and the contents were mixed by shaking the vials thoroughly with hands for 30 seconds. Then, the vials were placed into the wells of a Model Aqua Lytic COD Reactor (ET 108) and heated at 150 °C for 2 hr. Every 10 min, the vials were removed and shaken thoroughly by hand to combine condensed water and clear insoluble matter from the walls of the vials. After 2 hours, the vials were removed from the reactor and cooled to room temperature. Absorbance of the vial contents was measured at 600 nm using Aqua Lytic spectrometer (Germany).

The antifouling property was measured by calculating the flux recovery (FR) as follows:

$$FR(\%) = \left(\frac{J_1}{J_0}\right) \times 100 \quad (6)$$

where J_0 and J_1 are the pure water of virgin and fouled membrane. Generally, the fouling of UF membrane is caused by reversible and irreversible ones. Reversible fouling (R_r) can be easily removed by DI water washing. In any case, irreversible fouling (R_{ir}) remains after washing unless more drastic chemical cleaning is applied. R_r and R_{ir} are calculated by the following equations:

$$R_r = \left(\frac{J_1 - J_p}{J_0}\right) \times 100 \quad (7)$$

$$R_{ir} = \left(\frac{J_0 - J_1}{J_0}\right) \times 100 \quad (8)$$

The total fouling ratio (R_t) is the sum of reversible and irreversible fouling and also calculated as following:

$$R_t = \left(1 - \frac{J_p}{J_0}\right) \times 100 \quad (9)$$

Here, J_p is flux of landfill leachate.

RESULTS AND DISCUSSION

1. Physicochemical Properties of the WO_3/PSf Membrane

The filtration performance is mainly related to the surface properties of the synthesized membrane. The surface chemistry of the neat and modified PSf membrane was evaluated via ATR-FTIR, and the results are illustrated in Fig. 2. It seems that both peaks at 1,010 cm^{-1} and 1,242 cm^{-1} were attributed to the C-O asymmetric stretch. Also, peaks at 1,296 cm^{-1} and 1,157 cm^{-1} corresponded to the symmetric stretch slogans' (S=O). The adsorption bands at 694 cm^{-1} and 833 cm^{-1} were assigned to C-H aromatics. An absorption band at 3,394 cm^{-1} corresponded to the O-H stretch. The peak at 1,319 cm^{-1} was also assigned to the CSO2C asymmetric stretch. Both of peaks at 1,488 cm^{-1} and 1,581 cm^{-1} were attributed to the C_6H_6 ring stretch [34]. In the spectra of WO_3/PSf membrane, a new peak appearing at 918 cm^{-1} was assigned to the W=O stretching vibration band [35].

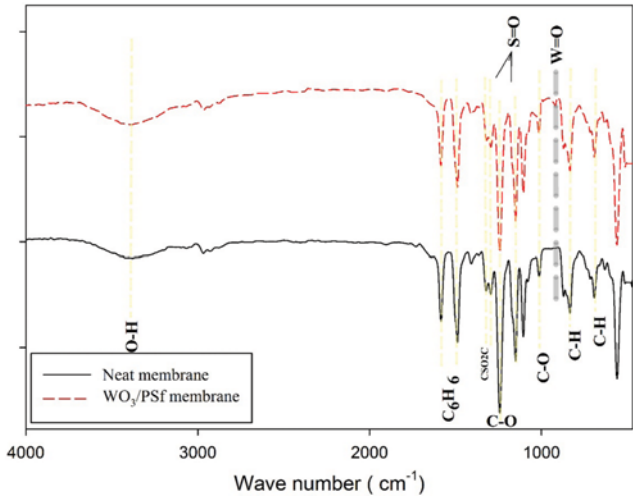

Fig. 2. FTIR spectra of Neat and modified membrane.

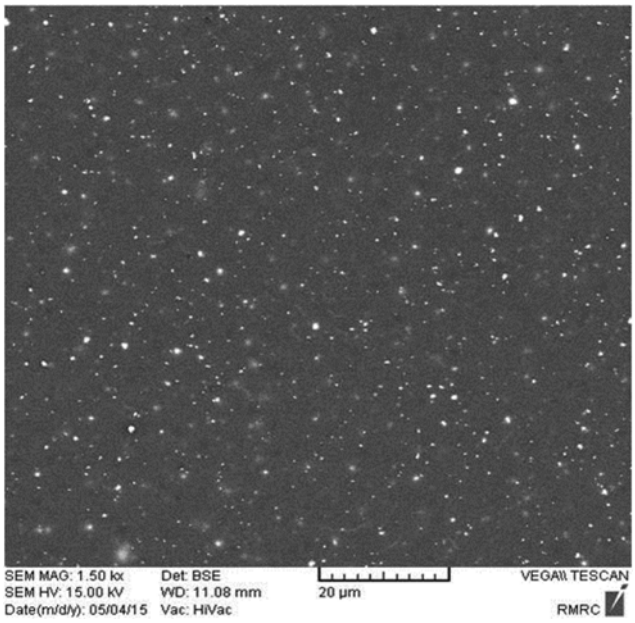

Fig. 3. SEM image of modified membrane (WO_3-1%).

To investigate the morphological study and particle size distribution of synthesized membranes, SEM and AFM analyses were carried out. Fig. 3 shows the quality of dispersion and distribution of nanoparticles on membrane surface. The bright dots observed on the membrane surface were attributed to WO_3 nanoparticles, and the more opaque ones were merged into the membrane. The surface SEM images of modified and neat membrane are shown in Fig. 4. The surface image of the neat membrane showed fully uniform surface without any defects and cracks. This is the usual morphology for the commercial dense asymmetric membrane. It can be considered that WO_3 nanoparticles were also distributed on the membrane surface. The size of these nanoparticles on the membrane surface was estimated about 70-150 nm at higher magnification. EDX analysis was used to identify the chemical components of the modified membranes. The elements of C, O, W and S were detected and shown in Fig. 5. Note that the sharp peak of Au element in this diagram was caused by the coated aurum on the sample and is irrelevant to the elemental analysis of the membranes.

The cross-sectional SEM images of the neat and modified membranes by WO_3-1% are demonstrated in Fig. 6. All membranes exhibited typical asymmetric structures with dense top layers. The neat membrane had both finger-like and sponge-like structures. It shows that the morphology of the modified membrane changed to finger-like by adding WO_3 nanoparticles. In contrast to the neat membrane, the finger-like pores for modified membrane were also extended along the membrane thickness. The hydrophilic nature of WO_3 accelerates the mass transfer rate between the solvent and the non-solvent during phase inversion [36]. Also, some amount of WO_3 may diffuse into the coagulation bath and act as the hydrophilic and pore forming agents during the phase inversion. The presence of WO_3 nanoparticles in the casting solution led to the interconnection between the pores due to the migration of WO_3

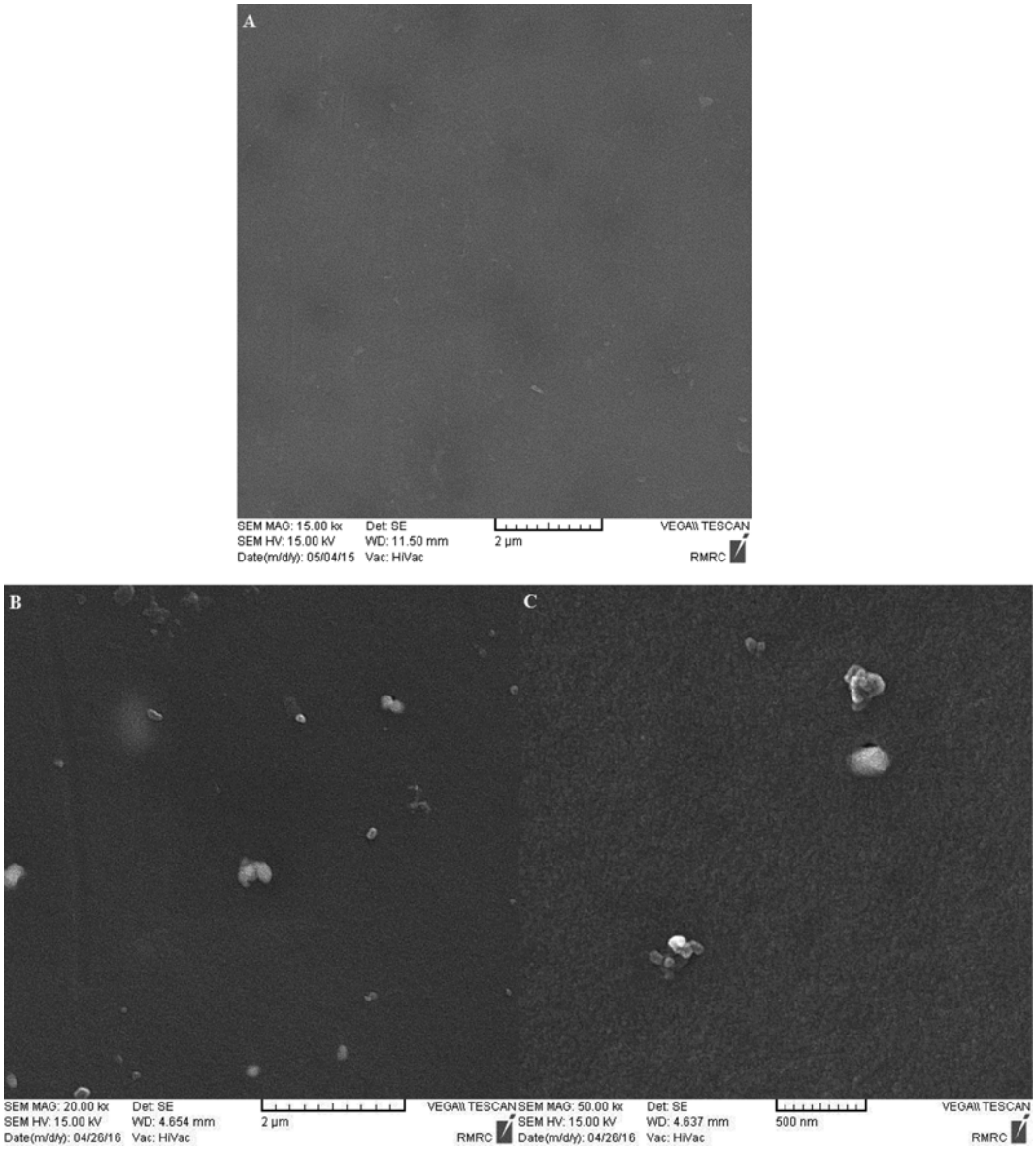

Fig. 4. SEM images of membrane surface (A) Neat membrane, (B) WO_3 nano particles on the membrane surface, (C) Magnification of modified membrane (WO_3-1%).

nanoparticles, and consequently the pores ran through to form the long finger-like during the membrane formation. As a general law, the porosity can rise by enlarging the finger-like cavity or adding cavity sets. It means that the finger-like structure has a higher porosity than the sponge-like [37]. Higher magnification of the SEM images of the neat and modified membrane in Fig. 6(C), (D) shows that the porosity of fully finger-like structure was evidently more than partial finger-like structure. This was quantified by measuring the weight of water saturated the pores. Results show that the weight of water that was saturating the modified pores with finger-like structure was more than the neat one with both finger and sponge structures (Table 3). Fig. 7 also shows the cross-sectional SEM images of top layer for neat and modified membrane. As can be seen, the shape of the top layer was different. The top layer of modified membrane became denser and thicker than its counterpart in membranes without additive. In addition, for neat membrane, a porous sponge structure of the top layer was observed.

The two- and three-dimensional surface AFM images of WO_3-1% and WO_3-2% as the modified membranes and neat membrane at a scan size of 5 µm×5 µm are shown in Fig. 8. In these images, the brightest area represents the highest point of the membrane surface, and the dark regions indicate valley or membrane pores. The roughness parameters of the membrane surface were increased by adding the WO_3 nanoparticles as listed in Table 2. These might be due to the presence of nanoparticles on the membrane surface [38].

The hydrophilic property of the PSf/WO_3 membrane (WO_3-1% and WO_3-2%) was characterized and compared with the neat PSf membrane through the measurement of water contact angle. The contact angle of neat and modified membrane under UV radia-

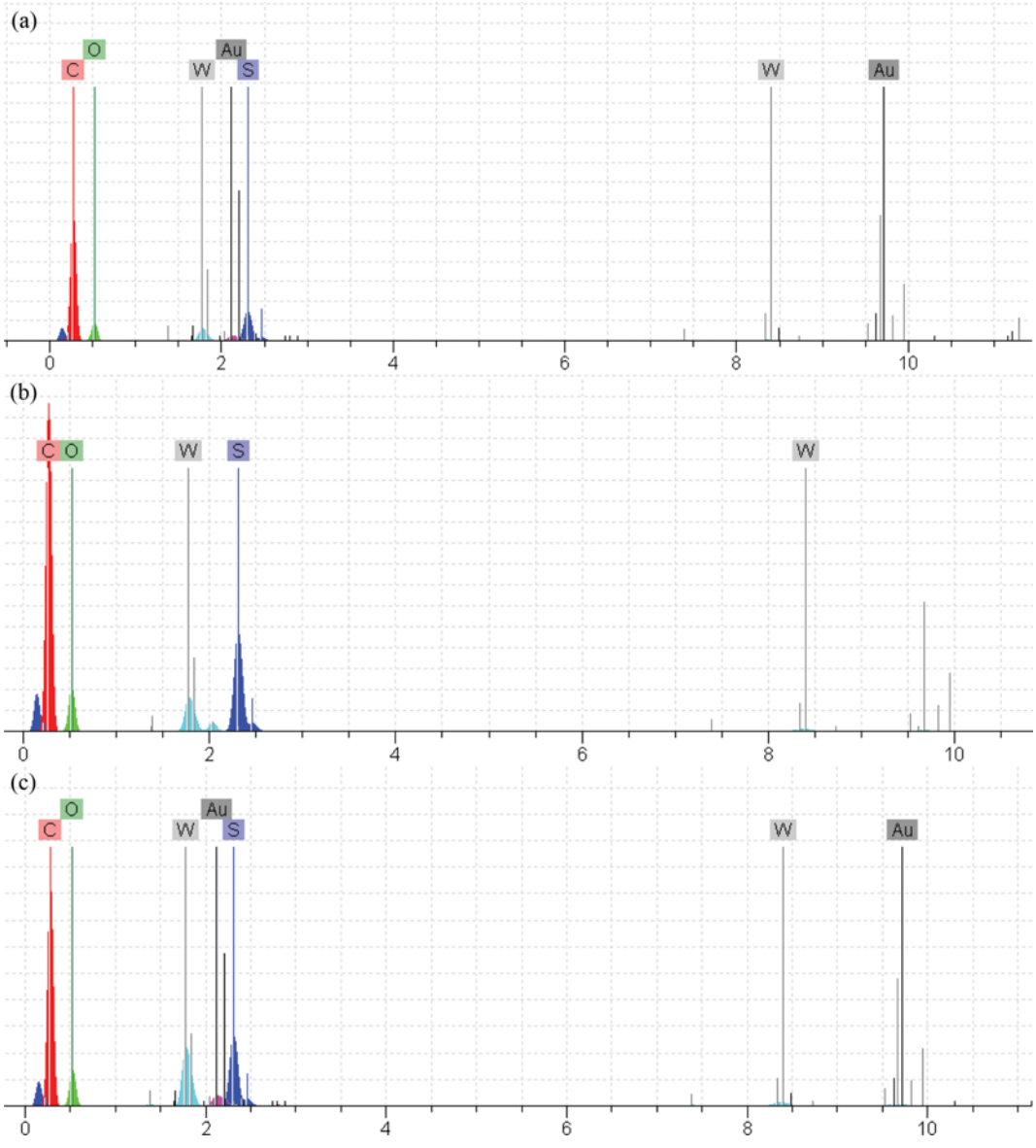

Fig. 5. EDX analysis of (a) WO_3- 0.5% (b) WO_3- 1% (c) WO_3- 2% membrane.

tion were also measured and reported. Fig. 9 shows that the contact angle of membranes decreased with increasing the WO_3 nanoparticles loading in the casting solution. It can be concluded that the surface hydrophilicity was improved by increasing the nanoparticles concentration. It might be attributed to the hydrophilic nature of WO_3 nanoparticles [39]. In addition, the modified membrane surface became more hydrophilic by increasing the loading nanoparticles when exposed to UV light, while the contact of neat PSf membrane remained almost constant. When the modified membrane surface was irradiated with UV light, parts of the organic compounds on the WO_3 surface were photocatalytically decomposed. The reduction of hydrogen bond network between the H_2O molecules by UV light irradiation on the WO_3 surface was closely related to the surface tension decline of the H_2O. These changes in the surface tension of H_2O can be associated with a thermodynamic driving force. This phenomenon can be justified by increasing the density of the hydroxyl groups on the WO_3 by UV light irradiation. The mechanism of the photocatalytic and self-cleaning properties of WO_3/PSf membrane is depicted schematically in Fig. 10. WO_3 nanoparticles as a semiconductor have a valence band and a conduction band. They are separated by a free region of energy levels. This region is denoted as the band gap energy. When semiconductor is irradiated with UV or solar light, it absorbs energy that is greater than its band gap energy, and consequently causes to transfer electrons. This transfer of an electron results in the generation of a hole (h+) in the valence band. These electrons and holes separate and transfer to the WO_3 surface participating in oxidation and reduction reactions. Hydroxyl radicals, which are the products of the reaction between valence band holes and water, can react with air humidity to create a hydroxyl group [40].

In modified membrane, photo-generated holes first produce OH radicals, which can result in an increase of OH groups. This

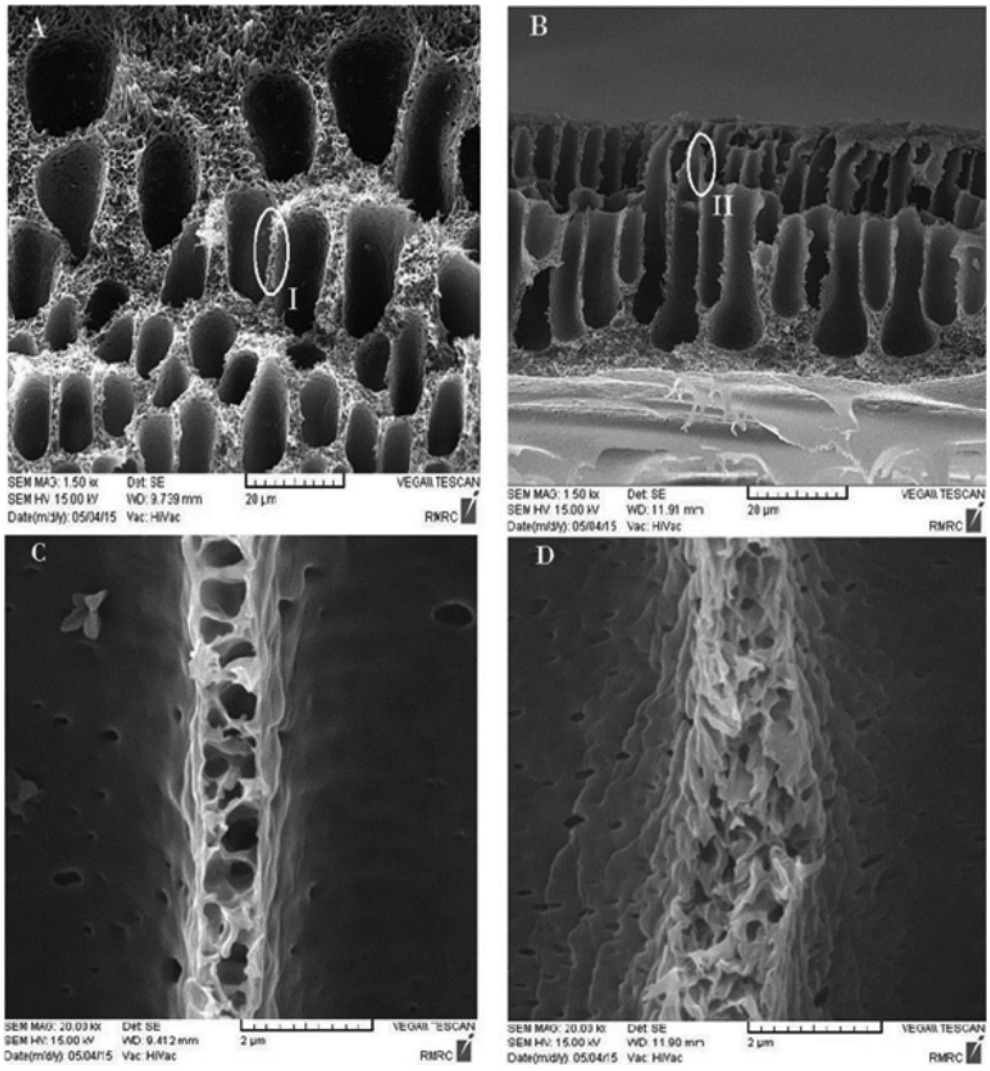

Fig. 6. SEM images of cross-section (A) Neat membrane (B) modified membrane (WO_3- 1%) (C) Magnification of section I (D) Magnification of section II.

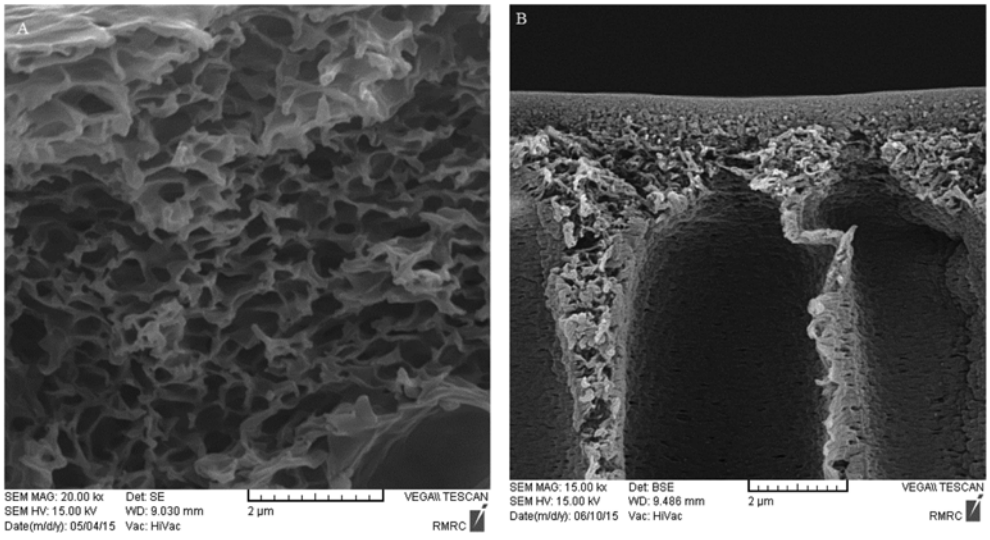

Fig. 7. SEM images of cross-section of upper part (A) Neat membrane (B) modified membrane (WO_3-1%).

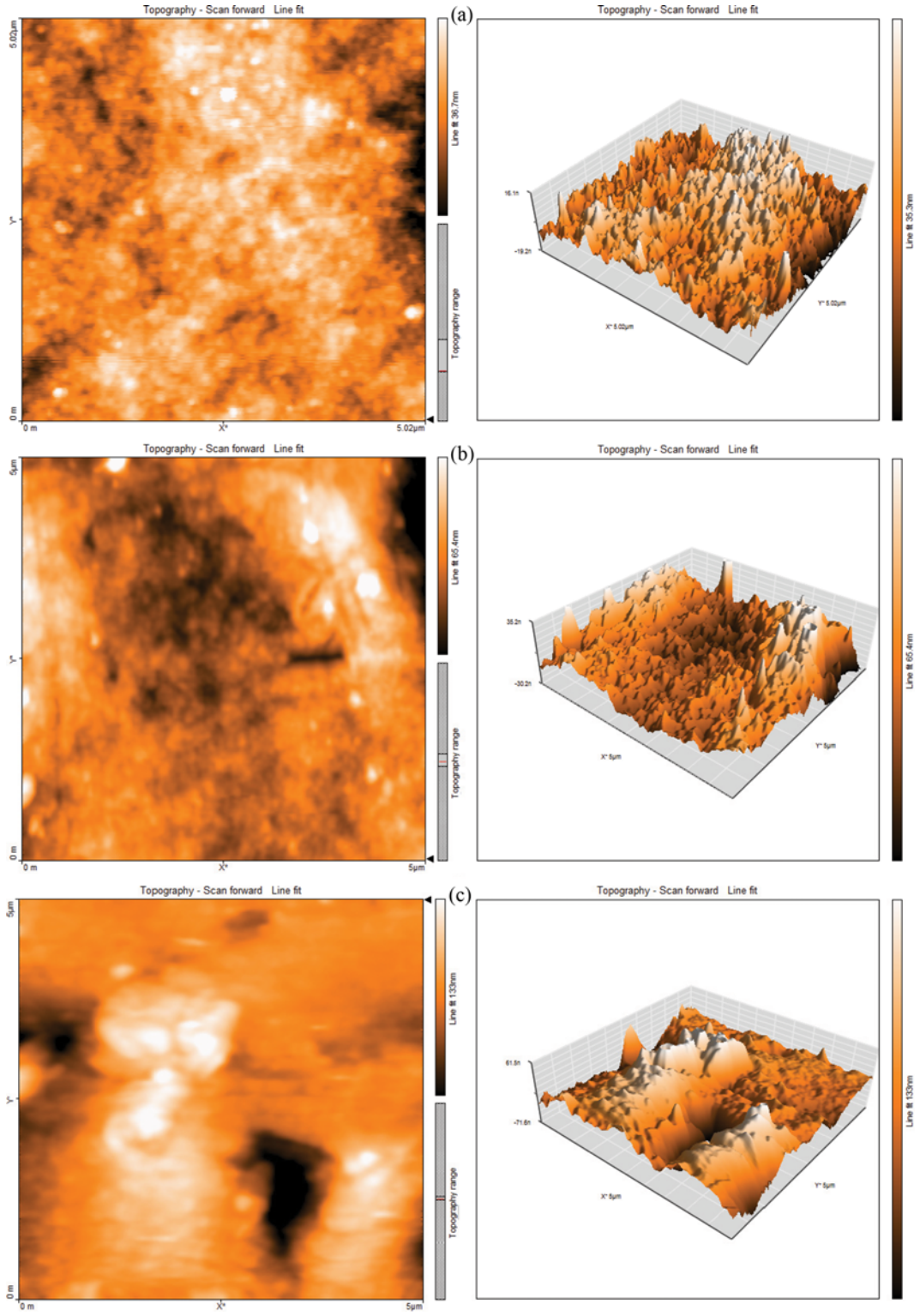

Fig. 8. The two and three-dimensional surface AFM images of (a) Neat, (b) WO_3-1%, (c) WO_3-2% membrane.

increases the surface energy, which leads to the decrease of contact angle, and forming a super-hydrophilic surface as a result [41]. The 1% PSf/WO_3 membrane also showed higher wettability as compared to the neat membrane. This is due to increase in hydrophilicity by WO_3 addition.

2. Structural Properties of the WO_3/PSf Membrane

The structural characteristics of the membrane such as pore size and porosity have direct impact on membrane fouling. Membranes with very small pores would be expected to "trap" fewer particles than membrane with surface, which have pores of the same

Table 2. Membrane surface roughness

Membrane	Roughness		
	S_a (nm)	S_q (nm)	S_z (nm)
WO_3-2%	18.74	26.22	216.42
WO_3-1%	9.67	12.63	120.89
Neat	5.12	6.41	57.78

size as the macrosolutes, and particles. Porosity and pore size of the modified and neat membranes were calculated and shown in Table 3. The porosity was enhanced by increasing the WO_3 nanoparticles content, which acted here as a porous agent. In fact, after the certain time of exchange between solvent and nonsolvent, WO_3 nanoparticles tend to diffuse to the coagulation bath until the solution becomes thermodynamically unstable and remixing takes place. Although, the porosity of WO_3-0.5% is lower than neat membrane

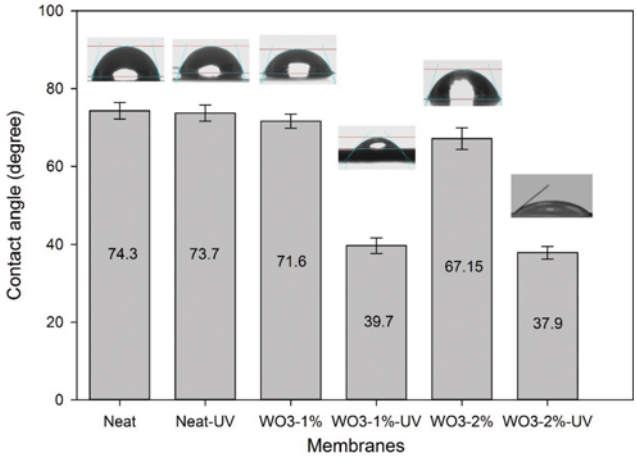

Fig. 9. Contact angle values of modified and neat membranes. The error bars are standard deviation.

Table 3. Summary of characterization of Neat, WO_3/PSf and membranes containing TiO_2. The numbers in parentheses are standard deviation

Membrane	Characterization	Pore size (nm)	Porosity (%)	Contact angle (°)		Reference
				Without UV	With UV	
Neat		10.40 (±1.70)	28.41	74.30 (±2.10)	73.70 (±2.10)	The present work
WO_3/PSf	0.5% wt WO_3	8.73 (±1.50)	13.10	-	-	The present work
	1% wt WO_3	8.10 (±1.10)	49.20	71.60 (±1.80)	39.70 (±2.00)	The present work
	2% wt WO_3	7.72 (±1.15)	84.86	67.15 (±2.80)	37.90 (±1.60)	The present work
TiO_2/PSf	5% wt TiO_2	-	-	56	47	[57]
	10% wt TiO_2	-	-	54	44	
TiO_2/PSf	1% wt TiO_2	9.30	69.40	52.40	-	[1]
	2% wt TiO_2	8.90	80.30	41.40	-	
TiO_2/PSf	1% wt TiO_2	6.90	60.30	52.60	-	[58]
	2% wt TiO_2	6.30	76.50	49.40	-	
TiO_2/PVDF	1% wt TiO_2	>35	-	68.70	-	[59]
	4% wt TiO_2	>25	-	65.10	-	

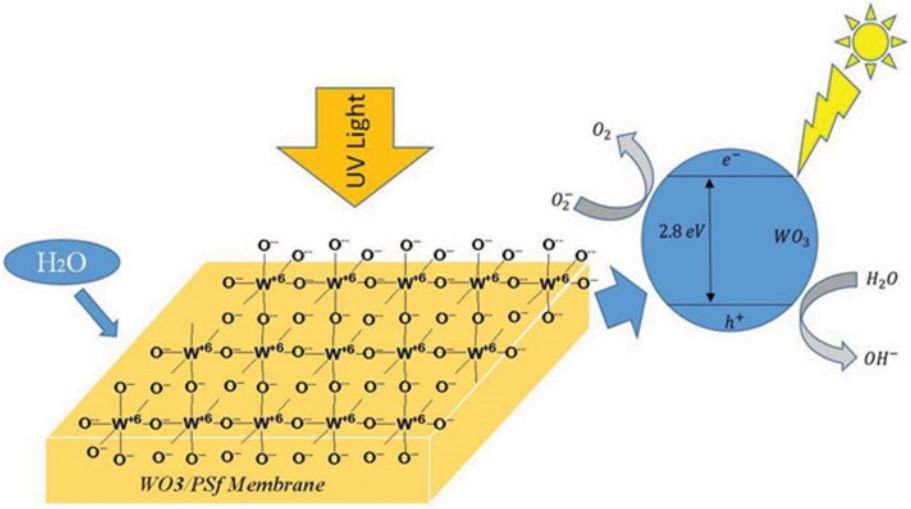

Fig. 10. Schematic of the photocatalytic and self-cleaning process of WO_3/PSf membrane.

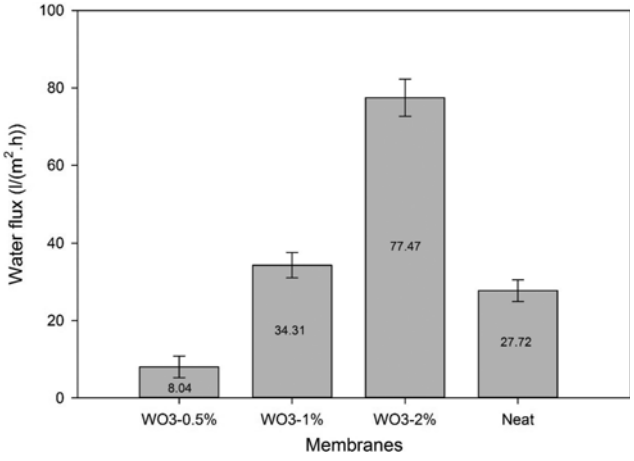

Fig. 11. Water flux of neat and modified membranes. The error bars are standard deviation of the mean.

due to slow precipitation rate [42]. The modified membrane indicates the narrower pore size distribution than the neat membrane. Fig. 6(C), (D) confirms these statements. As can be seen, the pore size of the modified membranes is smaller than neat one and their porosity is more than the neat PSf membrane. The WO_3 concentration decelerates the exchange between solvent and non-solvent during the phase separation process, and finally ceases to form a smaller pore size [43]. Fig. 11 shows the water flux of neat and modified membranes. Some structural parameters such as pore size, porosity, hydrophilicity and roughness are effective on the water flux, since by increasing each of these parameters, the water flux is improved [44,45]. Although the pore size of the UF membrane was decreased by increasing the WO_3 nanoparticles, the porosity, hydrophilicity and roughness were enhanced. It seems that the effect of these three parameters was dominant compared to the pore size and ultimately the water flux improved by increasing the WO_3 nanoparticles.

A comparison between WO_3 nanoparticle (the present work) and TiO_2 as a common photocatalytic additive for inducing self-cleaning property of the ultrafiltration PSf membrane is shown in Table 3. Generally, the rejection improves by decreasing the pore size and the flux enhances via increasing the porosity, which is desirable in membrane treatment. Regarding Table 3, membranes containing 1% and 2% WO_3 nanoparticles had favorable pore size and porosity, which can be appropriate performance in treatment. Also, the membrane containing WO_3 nanoparticles showed good hydrophilicity in comparison to membranes including nano TiO_2 after UV radiation.

3. Self-cleaning Property of the WO_3/PSf Membrane

3-1. Effect of Adding Nanoparticles on Self-cleaning Property

The experimental results of the landfill leachate flux for all modified membranes with and without UV are shown in Fig. 12. The membranes were immersed in distilled water for 15 min before each test. The organic matter is a more important factor in creating fouling and cake formation on the membrane [46]. The organic compound with a larger size is deposited on the surface and forms a layer so that its thickness is increased by filtration time. Thus, the permeate flux is decreased by filtration time. Fig 12(a) shows that

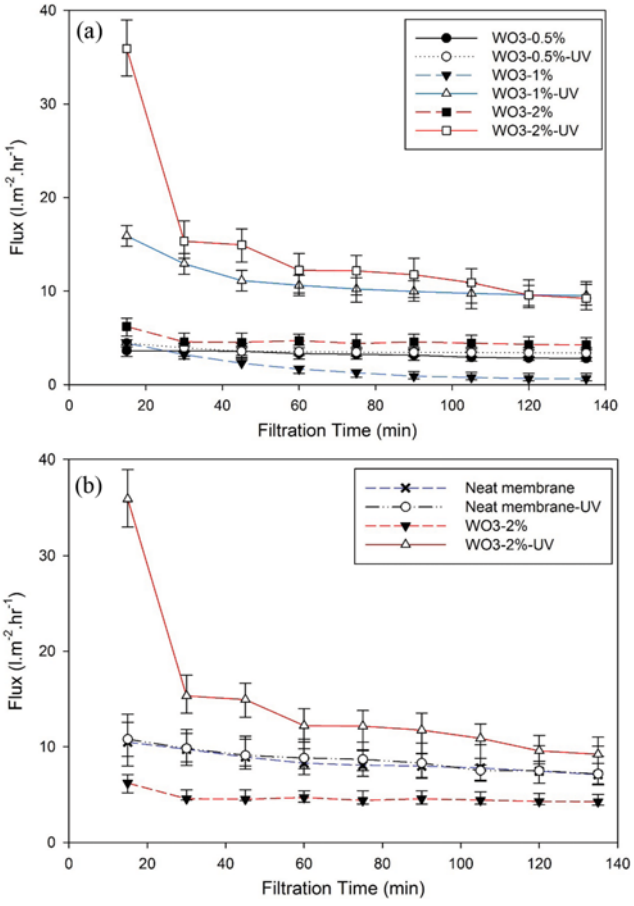

Fig. 12. Landfill leachate flux for (a) different WO_3 concentration (b) WO_3-2% and neat membrane. The error bars are standard deviation.

the flux of WO_3/PSf membranes with UV radiation were higher than without ones in all three concentrations of WO_3. As a result, the WO_3 nanoparticles were not revived without UV radiation. Indeed, the photocatalytic and ultrahydrophilicity properties and totally the self-cleaning property were not created on the membrane surface without UV radiation. There is a brilliant relationship between hydrophilicity and photocatalysis mechanisms on the self-cleaning property of the membrane surface. Hydrophilicity leads to the improvement in the photocatalytic property by adsorbing the OH groups on the surface. Photocatalysis also increases the hydrophilicity by decomposing the organic compounds on the surface. On the membrane containing WO_3 nanoparticles, water almost completely wets the membrane surface because of van der Waals forces and hydrogen bonds. Hence, by this mechanism the organic compounds have no chance of attaching to the surface and the membrane surface shows self-cleaning effects [47].

It can also be observed that the flux of landfill leachate is more enhanced by increasing the concentration of WO_3 in the membrane. This is because of better hydrophilic property and larger porosity and roughness by increasing WO_3 nanoparticles. Consequently, the highest flux is obtained for the membrane containing 2% wt WO_3. Fig. 12(b) shows the landfill leachate flux for neat and 2% wt WO_3 membrane with and without UV radiation. The

flux of landfill leachate using 2% wt WO_3 membrane is higher compared to the flux of the neat membrane. This is due to hydrophilicity and photocatalytic properties of WO_3 particles radiated on the membrane surface by UV irradiation as mentioned before. The photocatalytic property of WO_3 causes a high proportion of hydroxyl groups to be adsorbed onto the surface and decompose the organic compounds. As shown in Fig. 12(b) the landfill leachate flux of the modified membrane without UV is lower than the neat membrane. The WO_3 nanoparticles on the membrane surface without UV radiation blocked the fluid passage and decreased the average pore size. As a result, the flux decreased. Also, it is evident that the flux of neat membrane did not have any significant differences with or without UV radiation. It demonstrates that the UV radiation on the membrane surface is not enough for creating the self-cleaning property.

3-2. Comparison between the Effect of Self-cleaning Property and Shear Force on Fouling

A comparison between the effect of using WO_3 nanoparticles in order to induce self-cleaning property and shear force (as an operating parameter) on fouling phenomenon was investigated. The transmembrane pressure and the shear force are the hydrodynamic parameters' effect on permeate, which in turn depends on the cross-flow velocity [48]. The cross-flow velocity or shear force was controlled by adjusting the recirculation rate. Fig. 13 shows the landfill leachate flux of long-term filtration of WO_3-2% in 0.027 m/s, 0.045 m/s, 0.06 m/s and 0.09 m/s feed velocity. Considerations of the volumetric flow rate, the Reynolds number showed that the flow was laminar at all the flow velocities. It reveals that the flux is increased with increasing the feed velocity, which is due to the removal of the cake layer at high shear rates [49]. It also indicates that the effect of UV irradiation on membrane surface is the dominant factor in lower velocities. However, at high velocities shear force is prevalent on UV irradiation; the usual transmembrane pressure in UF systems is between 1-5 bar [50], which includes low velocities. Therefore, it can be concluded that the UV irradiation is reliable factor in UF systems having photocatalytic nanoparticles in their membrane matrix.

4. Antifouling behavior of the WO_3/PSf Membrane

Fig. 12(a), (b) also shows the long-term ultrafiltration of landfill leachate. The typical flux decline during ultrafiltration can be observed. Macromolecules of organic compounds in feed deposit on or within the membrane and the flux reduce because of pore blocking. The main reason for flux decline in long-term test is cake formation because of accumulation of organic compounds on the membrane surface over time. For more details, the flux decline rates were calculated in each synthesized membrane and summarized in Table 4. By radiating UV on the membrane, the rate of flux decline decreases in comparison to without UV radiation. The WO_3 nanoparticles have photocatalytic property and they cause to decompose the organic pollutants from the membrane surface. Photocatalytic property is also activated by UV radiation. The flux decline of WO_3 nanoparticles with UV radiation was higher than without nanoparticles. It may be attributed to the high roughness that can be seen in AFM images of modified membrane in comparison to neat one.

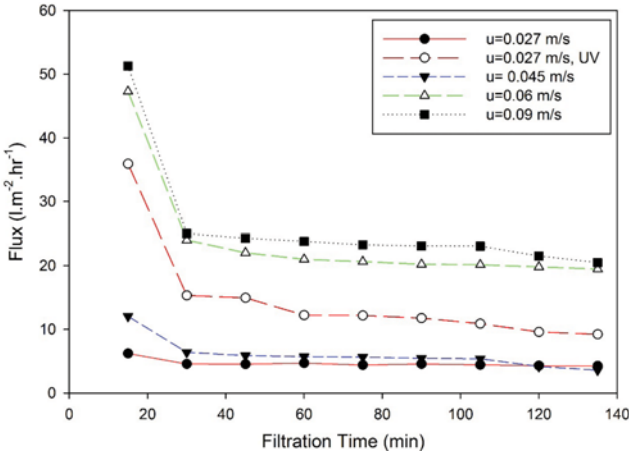

Fig. 13. Landfill leachate flux in different velocities.

Table 4. Flux decline rates

Membrane	Flux decline rate (%)	
	Without UV	With UV
Neat	27.26	27.16
WO_3-0.5%	22.75	14.23
WO_3-1%	80.17	26.24
WO_3-2%	6.91	39.41

Under the scanning electron microscope (SEM), membrane surface for the neat and modified membranes before and after UV irradiation and after filtration was observed (Fig. 14). Comparison of Fig. 14(A) with Fig. 14(B) and Fig. 14(D) with Fig. 14(E) indicates that the membrane surfaces have no major change before and after UV treatment. This reveals that UV irradiation is not able to degrade membrane structure [22]. As shown in Fig. 14(C) many contaminants particles are adsorbed on the surface of neat membrane. Agglomerate contaminants can be detected in the local of membrane surface. Also, contaminant particles adsorbed on the modified fouled membrane surface are smaller than neat ones and the contaminated layer has more roughness on the neat membrane surface (Fig. 14(F)). These observations are justifiable by following explanations: On the one hand, the increment of the membrane's hydrophilicity leads to different amounts of contaminants adsorption on the membrane surface; on the other hand, the WO_3 after UV irradiation destroys organic matter of the cake deposit into small organic matter by hydroxyl radicals generation, due to its photocatalytic property [51,52].

Landfill leachate filtration was performed to evaluate the antifouling behavior of the synthesized membranes. Table 5 lists the flux recovery ratio (FR) of the membranes with and without UV radiation. It shows that membranes had stronger antifouling abilities by UV radiation, and the amount of FR was increased by increment the WO_3 nanoparticles in the membrane. The obtained higher recovery ratios for the modified membranes also proved that the absorbed fouling layers on the membranes were relatively thin and easily removable. Moreover, the increment of flux recoveries may be attributed to the higher membrane surface hydrophilicity as a consequence of enhancing nanoparticles. To further

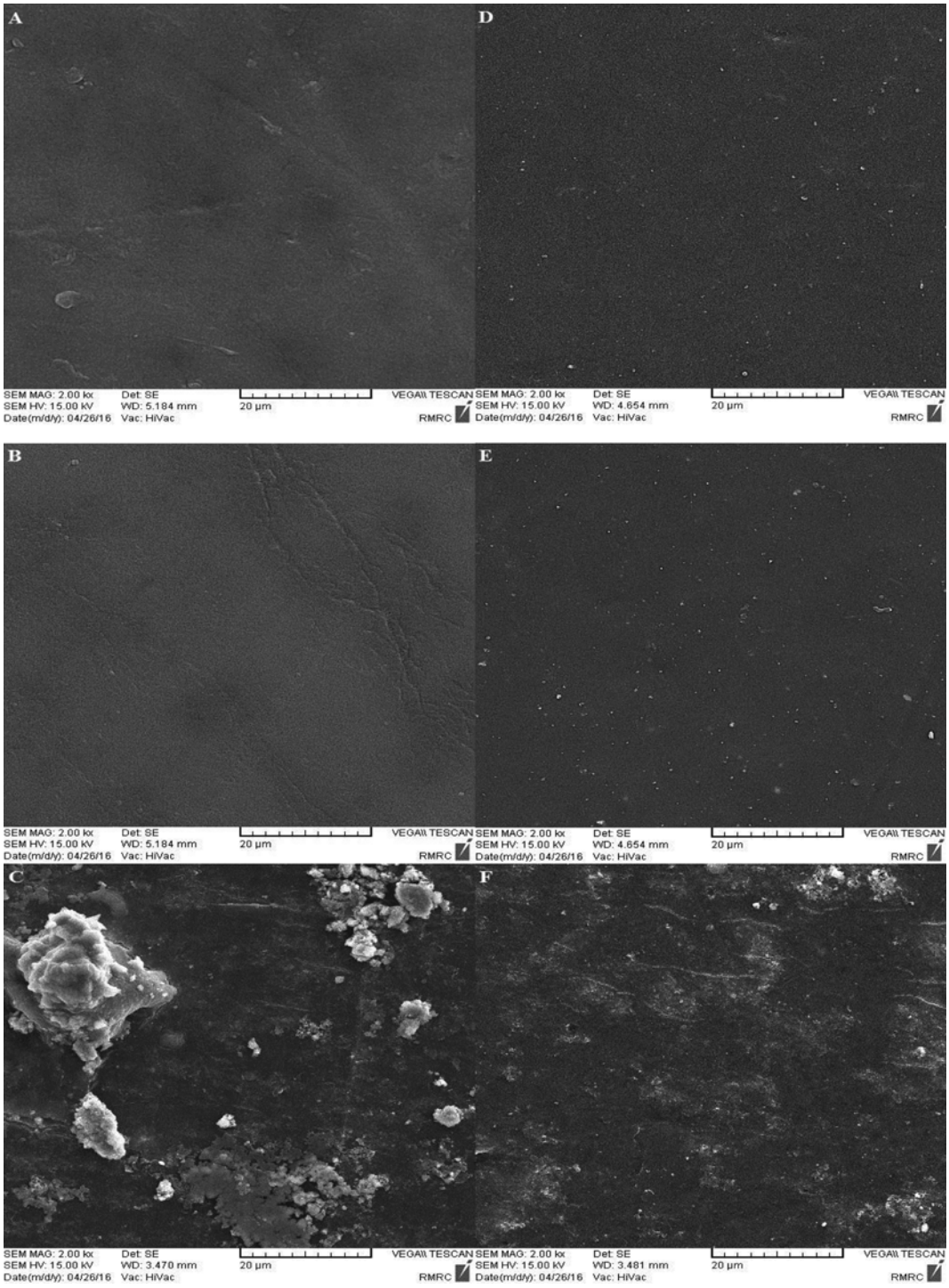

Fig. 14. SEM images of membrane surface (A) neat membrane before UV irradiation (B) neat membrane after UV irradiation (C) fouled neat membrane (D) modified membrane before UV irradiation (E) modified membrane after UV irradiation (F) fouled modified membrane.

investigate the fouling, reversible resistance (R_r), irreversible resistance (R_{ir}) and total resistance (R_t) were measured and summarized in Table 5. R_{ir} is attributed to a pore blocking effect and the R_r is imputed to the cake filtration [53]. R_t is the sum of these parameters and shows the total resistance of fouling against landfill leachate flux. As a result, the flux recovery of all the synthesized membrane was increased by decreasing the fouling resistance. The fouling resistance was decreased by radiating the UV on the membrane. This may be attributed to the decomposition of the agglomeration of organic matters in the membrane pores after UV radiation. The results also showed that the contribution of irreversible resistance was more than the reversible one in the total resistance. The

Table 5. Flux recovery ratio, total resistance, reversible resistance and irreversible resistance of different membranes with and without UV radiation

Membrane	R_t		R_r		R_{ir}		FR (%)	
	Without UV	With UV	Without UV	With UV	Without UV	With UV	Without UV	With UV
WO_3-0.5%	0.5130	0.4490	0.0620	0.0220	0.4510	0.4270	54.82	57.21
WO_3-1%	0.9241	0.5361	0.0797	0.0671	0.8444	0.4690	15.55	58.49
WO_3-2%	0.5937	0.5362	0.2033	0.1853	0.3903	0.3509	59.96	64.90
Neat	0.6275	0.6106	0.1372	0.1255	0.4903	0.4851	50.96	51.48

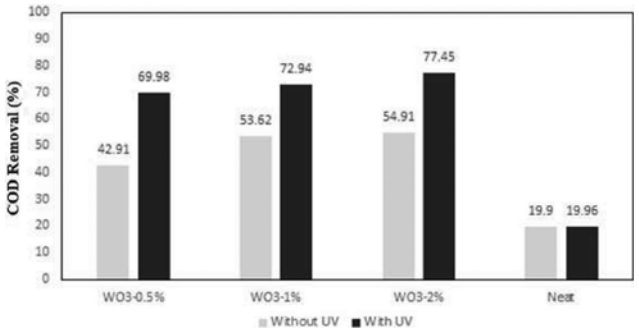

Fig. 15. COD removal of different membranes with and without UV radiation.

maximum flux decline was obtained for WO_3-1% membrane without UV radiation because of the maximum amount of resistance [54]. As seen in Table 5, the value of R_r was increased, and consequently the amount of R_{ir} was decreased for WO_3-2% under UV light. Regarding R_r attributed to the formation of cake, the increase of cake may be due to the R_r increment. As a general rule, when R_t increases and R_{ir} decreases, the membrane shows better surface properties and performance in terms of fouling [55]. Furthermore, a considerable amount of nanoparticles may exist in the surface pores due to the higher loading of WO_3 nanoparticles. They cause to clean and reduce the pollution inside the holes by reflecting UV.

The chemical oxygen demand (COD) of the feed and permeate were measured; the COD removal of the synthesized membranes is shown in Fig. 15. The COD of landfill leachate selected as a feed was 12,420 mg/*l*. The COD removal of synthesis membranes was increased by increasing the WO_3 nanoparticles. In fact, nanoparticles reduced the pore size distribution (Table 3), and consequently the organic compounds with smaller size passed the membrane. This led to reduction in the amount of organic compounds in permeate and the COD was decreased. In addition, the removal of organic compounds in WO_3-2% was more than others before and after UV irradiation. The COD of landfill leachate by WO_3-2% membrane was decreased from 12,420 mg·l^{-1} to 2,800 mg·l^{-1}. The COD removal of all modified membrane was also increased by UV radiating because of a photocatalytic property of WO_3 [56].

CONCLUSION

To create photocatalysis self-cleaning membrane, WO_3 nanoparticles were added to polysulfone UF membranes. Photocatalytic and ultrahydrophilicity properties were carried out by UV radiation. The following conclusions can be drawn from the experimental results.

The photocatalysis self-cleaning polysulfone membranes were prepared by using WO_3 nanoparticles via phase inversion method. The modified PSf membranes exhibited significant self-cleaning photocatalytic properties. The membrane with 2% WO_3 showed better antifouling/self-cleaning ability as compared to the other modified and neat PSf membranes.

Membrane surface modification with WO_3 nanoparticles without UV radiation did not create self-cleaning property. The reason is that WO_3 particles may not revive without UV radiation. Radiation of UV light on the surface of neat membrane did not significantly affect the flux of it.

Wettability of the membranes was improved by increment of WO_3 content, so higher pure water flux was observed at higher WO_3 nanoparticles concentrations.

Membrane fouling resistance decreased with an increase in the nano WO_3 concentration, and for this reason the landfill leachate permeate increased. The total resistance also decreased after UV radiation for each modified membrane. In addition, UV irradiation did not have any effect on neat membrane.

By adding the WO_3, COD removal improved. The COD removal was increased because of the pore size reduction and the flux increment was due to the porosity improvement.

REFERENCES

1. Y. Yang, H. Zhang, P. Wang, Q. Zheng and J. Li, *J. Membr. Sci.*, **288**, 231 (2007).
2. A. Mollahosseini, A. Rahimpour, M. Jahamshahi, M. Peyravi and M. Khavarpour, *Desalination*, **306**, 41 (2012).
3. N. Ghaemi, S. S. Madaeni, A. Alizadeh, P. Daraei, M. M. S. Badieh, M. Falsafi and V. Vatanpour, *Sep. Purif. Technol.*, **96**, 214 (2012).
4. W. Gao, H. Liang, J. Ma, M. Han, Z.-l. Chen, Z.-s. Han and G.-b. Li, *Desalination*, **272**, 1 (2011).
5. S. P. Nunes and K.-V. Peinemann, *Membrane technology: in the chemical industry*, John Wiley & Sons (2006).
6. M. S. Muhamad, M. R. Salim and W.-J. Lau, *Korean J. Chem. Eng.*, **32**, 2319 (2015).
7. S. Hong and M. Elimelech, *J. Membr. Sci.*, **132**, 159 (1997).
8. A. Zularisam, A. Ismail and R. Salim, *Desalination*, **194**, 211 (2006).
9. H. Shon, S. Vigneswaran, R. B. Aim, H. Ngo, I. S. Kim and J. Cho, *Environ. Sci. Technol.*, **39**, 3864 (2005).
10. Y.-J. Won, J. Lee, D.-C. Choi, H.R. Chae, I. Kim, C.-H. Lee and I.-C. Kim, *Environ. Sci. Technol.*, **46**, 11021 (2012).

11. N. A. M. Nazri, W. J. Lau and A. F. Ismail, *Korean J. Chem. Eng.*, **32**, 1853 (2015).
12. G.-E. Chen, L. Sun, Z.-L. Xu, H. Yang, H.-H. Huang and Y.-J. Liu, *Korean J. Chem. Eng.*, **32**, 2492 (2015).
13. D. S. Wavhal and E. R. Fisher, *Desalination*, **172**, 189 (2005).
14. A. Reddy, D. J. Mohan, A. Bhattacharya, V. Shah and P. Ghosh, *J. Membr. Sci.*, **214**, 211 (2003).
15. J. K. Shim, H. S. Na, Y. M. Lee, H. Huh and Y. C. Nho, *J. Membr. Sci.*, **190**, 215 (2001).
16. M. Wang, L.-G. Wu, J.-X. Mo and C.-J. Gao, *J. Membr. Sci.*, **274**, 200 (2006).
17. C. Graf, S. Dembski, A. Hofmann and E. Rühl, *Langmuir*, **22**, 5604 (2006).
18. D. Rana and T. Matsuura, *Chem. Rev.*, **110**, 2448 (2010).
19. H. Bai and D. D. Sun, *Water Sci. Technol.: Water Supply*, **11**, 324 (2011).
20. H. Yamashita, H. Nakao, M. Takeuchi, Y. Nakatani and M. Anpo, *Nuclear Instruments and Methods in Physics Research Section B: Beam Interactions with Materials and Atoms*, **206**, 898 (2003).
21. K. Burgess, Self Cleaning Titania-Polyurethane Composites. 2007, Faculty of Graduates Studies, The University of Western Ontario, London.
22. A. Rahimpour, S. Madaeni, A. Taheri and Y. Mansourpanah, *J. Membr. Sci.*, **313**, 158 (2008).
23. V. A. Ganesh, H. K. Raut, A. S. Nair and S. Ramakrishna, *J. Mater. Chem.*, **21**, 16304 (2011).
24. H. Bai, X. Zhang, J. Pan, D. D. Sun and J. Shao, *Water Sci. Technol.: Water Supply*, **9**, 31 (2009).
25. P. Rios, H. Dodiuk and S. Kenig, *Surface Eng.*, **25**, 89 (2009).
26. G. Ren, Y. Gao, J. Yin, A. Xing and H. Liu, *J. Chem. Soc. Pakistan*, **33**, 666 (2011).
27. H. Wang, T. Lindgren, J. He, A. Hagfeldt and S.-E. Lindquist, *J. Phys. Chem. B*, **104**, 5686 (2000).
28. C. Santato, M. Odziemkowski, M. Ulmann and J. Augustynski, *J. Am. Chem. Soc.*, **123**, 10639 (2001).
29. O. J. Johansen and D. A. Carlson, *Water Res.*, **10**, 1129 (1976).
30. S. Madaeni and N. Ghaemi, *J. Membr. Sci.*, **303**, 221 (2007).
31. J.-F. Li, Z.-L. Xu, H. Yang, L.-Y. Yu and M. Liu, *Appl. Surf. Sci.*, **255**, 4725 (2009).
32. G. Wu, S. Gan, L. Cui and Y. Xu, *Appl. Surf. Sci.*, **254**, 7080 (2008).
33. L. Palacio, C. C. Ho and A. L. Zydney, *Biotechnol. Bioeng.*, **79**, 260 (2002).
34. A. Mushtaq, H. B. Mukhtar and A. M. Shariff, FTIR Study of Enhanced Polymeric Blend Membrane with Amines (2014).
35. T. Gavrilko, V. Stepkin and I. Shiyanovskaya, *J. Mol. Struct.*, **218**, 411 (1990).
36. V. Vatanpour, S. S. Madaeni, R. Moradian, S. Zinadini and B. Astinchap, *J. Membr. Sci.*, **375**, 284 (2011).
37. M. Shi, G. Printsypar, O. Iliev, V. M. Calo, G. L. Amy and S. P. Nunes, *J. Membr. Sci.*, **487**, 19 (2015).
38. N. Ghaemi, S. S. Madaeni, A. Alizadeh, H. Rajabi and P. Daraei, *J. Membr. Sci.*, **382**, 135 (2011).
39. M. Miyauchi, *Physical Chemistry Chemical Physics*, **10**, 6258 (2008).
40. A. L. Linsebigler, G. Lu and J. T. Yates Jr., *Chem. Rev.*, **95**, 735 (1995).
41. H. Irie and K. Hashimoto, *Photocatalytic active surfaces and photo-induced high hydrophilicity/high hydrophobicity*, in: Environmental Photochemistry Part II, Springer, 425 (2005).
42. D. Wang, K. Li and W. Teo, *J. Membr. Sci.*, **178**, 13 (2000).
43. H. Yu, X. Zhang, Y. Zhang, J. Liu and H. Zhang, *Desalination*, **326**, 69 (2013).
44. E. N. Laboy-Nieves, F. C. Schaffner, A. Abdelhadi and M. F. Goosen, *Environmental management, sustainable development and human health*, CRC Press (2008).
45. T. Wu, B. Zhou, T. Zhu, J. Shi, Z. Xu, C. Hu and J. Wang, *RSC Adv.*, **5**, 7880 (2015).
46. C. Liu, S. Caothien, J. Hayes, T. Caothuy, T. Otoyo and T. Ogawa, *Membrane chemical cleaning: from art to science*, Pall Corporation, Port Washington, NY, 11050 (2001).
47. K. Guan, *Surface and Coatings Technol.*, **191**, 155 (2005).
48. M. Cheryan, Ultrafiltration handbook, Technomic Pub. Co. (1986).
49. K. Sopajaree, S. Qasim, S. Basak and K. Rajeshwar, *J. Appl. Electrochem.*, **29**, 1111 (1999).
50. J. Mulder, *Basic principles of membrane technology*, Springer Science & Business Media (2012).
51. X. Zhang, A. J. Du, P. Lee, D. D. Sun and J. O. Leckie, *J. Membr. Sci.*, **313**, 44 (2008).
52. L. Yan, S. Hong, M. L. Li and Y. S. Li, *Sep. Purif. Technol.*, 66, 347 (2009).
53. T. Jiang, M. D. Kennedy, W. G. van der Meer, P. A. Vanrolleghem and J. C. Schippers, *Desalination*, **157**, 335 (2003).
54. G. Van den Berg and C. Smolders, *Desalination*, **77**, 101 (1990).
55. M. Peyravi, A. Rahimpour and M. Jahanshahi, *J. Membr. Sci.*, **473**, 72 (2015).
56. S. Chakrabarti and B. K. Dutta, *J. Hazard. Mater.*, **112**, 269 (2004).
57. S. You and C. Wu, *International Journal of Photoenergy*, 2013 (2013).
58. Y. Yang, P. Wang and Q. Zheng, *J. Polym. Sci. Part B: Polym. Phys.*, **44**, 879 (2006).
59. A. Rahimpour, M. Jahanshahi, B. Rajaeian and M. Rahimnejad, *Desalination*, **278**, 343 (2011).